JOURNAL OF GEOPHYSICAL RESEARCH, VOL. 108, NO. D24, 4781, doi:10.1029/2003JD003621, 2003

Clouds and sulfate are anticorrelated: A new diagnostic for global sulfur models

Dorothy Koch
NASA Goddard Institute for Space Studies, Columbia University, New York, New York, USA

Jeffrey Park
Department of Geology and Geophysics, Yale University, New Haven, Connecticut, USA

Anthony Del Genio
NASA Goddard Institute for Space Studies, Columbia University, New York, New York, USA

Received 21 March 2003; revised 29 September 2003; accepted 10 October 2003; published 24 December 2003.

[1] We consider the correlation between clouds and sulfate in order to assess the relative importance of cloud aqueous-phase production of sulfate, precipatation scavenging of sulfate, and inhibition of gas-phase sulfate production beneath clouds. Statistical analysis of observed daily cloud cover and sulfate surface concentrations in Europe and North America indicates a significant negative correlation between clouds and sulfate. This implies that clouds remove sulfate via precipitation scavenging and/or inhibit sulfate gas-phase production more than they enhance sulfate concentration through aqueous-phase production. Persistent sulfate/cloud anticorrelations at long timescales (8–64 days) apparently result from large-scale dynamical influences on clouds, which in turn impact sulfate. A statistical analysis of output from the general circulation model (GCM) of the Goddard Institute for Space Studies (GISS) shows weak coherence between sulfate and cloud cover. However, there is stronger anticorrelation between the model's sulfate generated by gas-phase oxidation and cloud cover. Sulfate/cloud anticorrelation in the GCM strengthens if we extinguish gas-phase sulfate production beneath clouds, as should happen since the oxidant OH is photochemically generated. However the only way to achieve strong anticorrelation between total sulfate and clouds is by correcting our treatment of aqueous-phase sulfate production. Our model, like many other global tracer models, released dissolved species (including sulfate) from clouds after each cloud time step rather than making release contingent upon cloud evaporation. After correcting this in the GISS model, more sulfate is rained out, the sulfate burden produced via the aqueous phase decreases to half its former amount, and the total sulfate burden is 25% lower. *INDEX TERMS:* 0305 Atmospheric Composition and Structure: Aerosols and particles (0345, 4801); 0320 Atmospheric Composition and Structure: Cloud physics and chemistry; 0365 Atmospheric Composition and Structure: Troposphere—composition and chemistry; 0368 Atmospheric Composition and Structure: Troposphere—constituent transport and chemistry; *KEYWORDS:* aerosol

Citation: Koch, D., J. Park, and A. Del Genio, Clouds and sulfate are anticorrelated: A new diagnostic for global sulfur models, *J. Geophys. Res.*, *108*(D24), 4781, doi:10.1029/2003JD003621, 2003.

1. Introduction

[2] The impact of sulfate aerosols on climate may be significant, but is subject to considerable uncertainty. The most straightforward impact is the "direct" effect (scattering of incoming solar radiation back to space). In terms of anthropogenic radiative forcing the direct effect may be -0.2 to -0.9 W m^{-2} [*Penner et al.*, 2001]. Potentially more significant (but much more uncertain) are the sulfate "indirect" effects on cloud radiative properties and lifetime, the first and second indirect effects, respectively. The first indirect effect is estimated to lie between 0 and -2 W m^{-2} [*Penner et al.*, 2001], but is highly uncertain; and the second indirect is too uncertain to assign a meaningful forcing range. Clouds are involved in both the production and removal of sulfate aerosols. Sulfate is almost entirely derived from oxidation of SO_2 either in the gas phase or aqueous phase (i.e., within cloud droplets). Gas-phase production will be suppressed beneath clouds due to reduced oxidant OH amounts. Sulfate, being highly soluble, is removed from the atmosphere mostly by precipitation scavenging, and to a lesser degree by dry deposition.

[3] Cloud processes generate, scavenge and are impacted by sulfate, but the overall relationship between them is poorly

0148-0227/03/2003JD003621$09.00

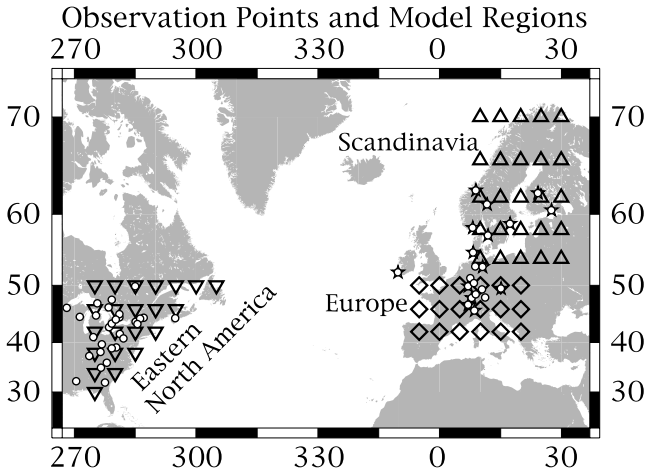

Figure 1. Map showing locations of sulfate surface concentration and ISCCP cloud cover observations (white circles); EMEP sites having precipitation and deposition information are marked with stars. Grid boxes used for the model calculations are triangles (Scandinavia), diamonds (Europe) and inverted triangles (North America).

known. Do cloudy conditions result in heavy sulfate production, or do clouds effectively clean the atmosphere of these aerosols? Do clouds inhibit gas-phase sulfate production significantly? If a single process dominates, we should observe strong correlation between clouds and sulfate, and a diagnostic phase relationship. If in-cloud production dominates, sulfate (or its rate-of-change) would be positively correlated with clouds. Negative correlation would result from scavenging and also from gas-phase production suppression beneath clouds.

[4] Previous studies using global sulfate models indicated that (model) sulfate generation occurs primarily in clouds. Tables summarizing these studies [see, e.g., *Koch et al.*, 1999; *Chin et al.*, 2000] suggest that most of the sulfate is produced in the aqueous phase (model estimates range from 64% to 89%). Most removal also occurs by wet deposition, typically around 80% (although the budgets are difficult to compare because some models identify rained-out sulfur as sulfate and some as SO_2), with the rest removed by dry deposition. Thus it appears that clouds play a highly significant role in both the generation and removal of sulfate aerosols. In the work of *Koch et al.* [1999], our global sulfur model indicated a slight tendency toward positive correlation between clouds and sulfate near source regions and anticorrelation in more remote regions.

[5] Given the level of uncertainty in modeling clouds and their interactions with the sulfur cycle, it is preferable to observe correlations in measurements. A number of efforts are now underway to tease out cloud/sulfate relations using satellite observations [*Schwartz et al.*, 2002; *Lohmann and Lesins*, 2002]. These studies must confront the problem of cloud-screening: the determination of where clouds end and aerosol haze begins. A further difficulty is distinguishing between sulfate and other aerosol types.

[6] Here we use a different approach to observe cloud-sulfate relations, by making use of the extensive surface concentration data sets that have been saved by European and North American networks. These data provide daily average concentrations of sulfate. To these we compare cloud satellite products which also have daily resolution. As we will show below, there is a strong negative correlation between clouds and sulfate. We use these results to test and correct our model's sulfur simulation.

2. Observations of Cloud-Sulfate Correlations

[7] In order to seek correlation between clouds and sulfate, we use daily average sulfate surface concentrations in Europe from the Cooperative Program for Monitoring and Evaluation of the Long Range Transmission of Air Pollutants in Europe (EMEP) [e.g., *Schaug et al.*, 1987] and in North America from the Eulerian Model Evaluation Field Study (EMEFS) [e.g., *McNaughton and Vet*, 1996]. We use 4 years of data from EMEP (1989–1992) and 1 year of data from EMEFS (1989–1990). We choose sites that have at least 20 days of sulfate data/month: 21 sites from EMEP and 31 sites from EMEFS. These locations are shown in Figure 1. We also made use of precipitation and sulfate deposition (i.e., in rainwater) data from the 15 of the EMEP sites that had this information (stars in Figure 1).

[8] Total cloud cover comes from the International Satellite Cloud Climatology Project (ISCCP, version D1) [e.g., *Stubenrauch et al.*, 1999; *Rossow and Schiffer*, 1999]. The satellite observations provide cloud parameters every 3 hours which we average to make 24-hour means. We chose to work with total cloud cover (results using cloud optical thickness were similar). We gathered time series with daily resolution of sulfate surface concentration and total cloud cover above the ground-based site.

[9] General features of the data series can be discerned from 4 months' data from one of the EMEP sites (Deuselbach

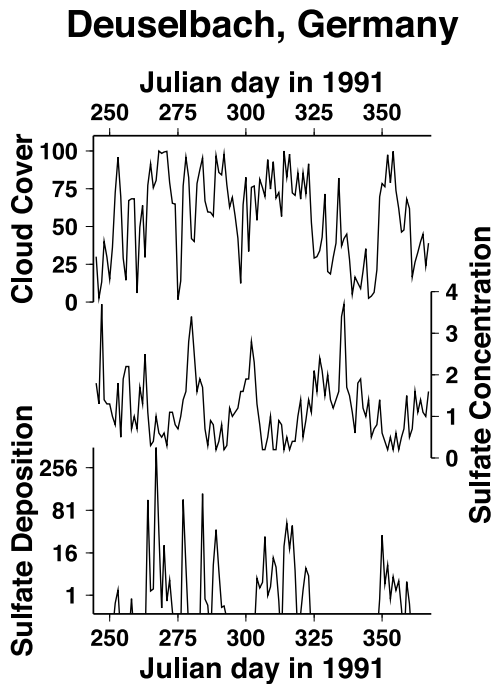

Figure 2. Time series of cloud cover (%), sulfate surface concentration (μg S/m^3) and sulfate deposition flux (μg S/m^2/d) at Deuselbach, Germany (49.8°N 7°E) for the last 125 days of 1991.

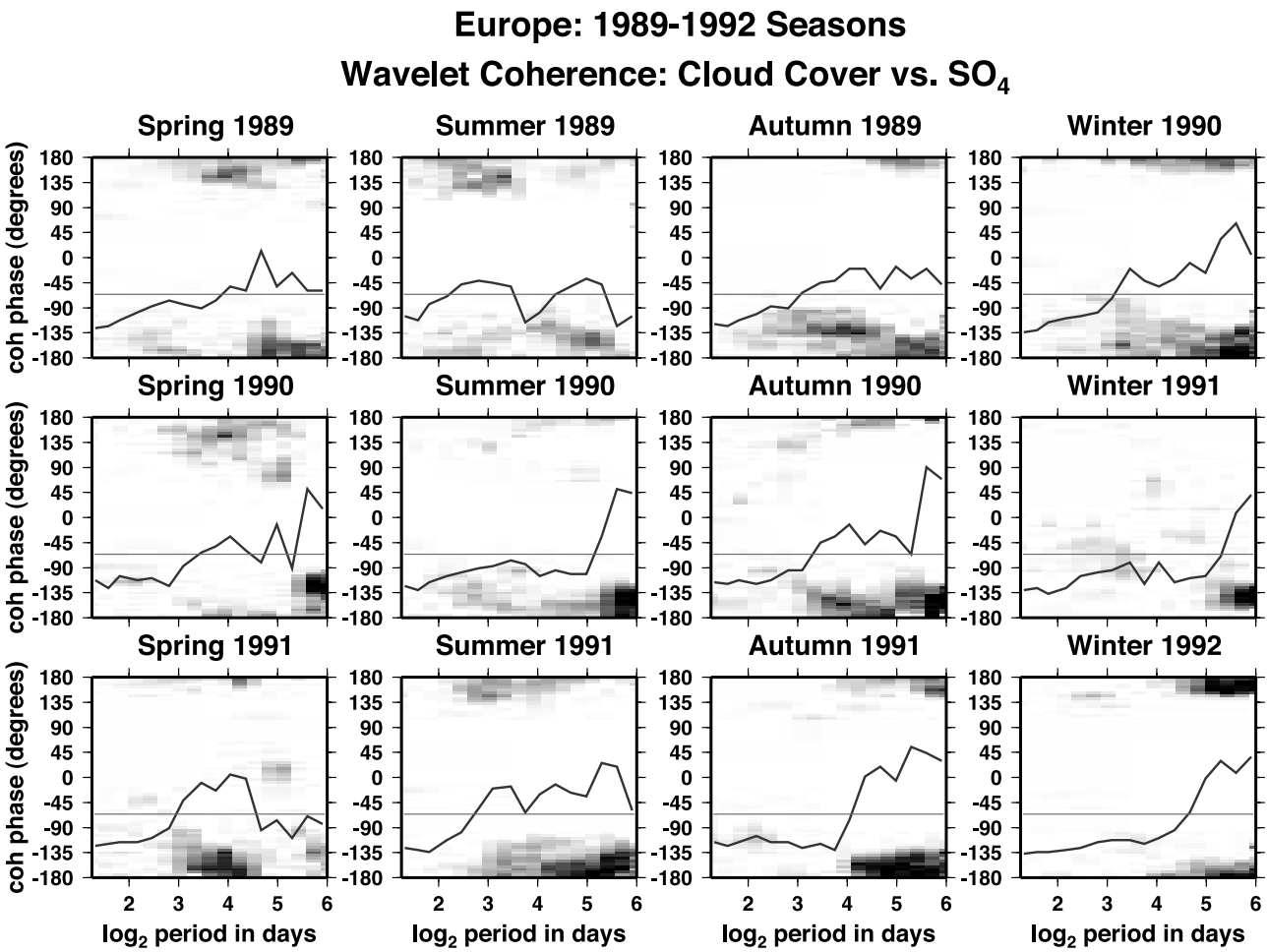

Figure 3. Squared coherence $\mathcal{C}^2$ between observed sulfate and cloud cover over Europe summed over each season for 1989–1992. On the log-period axis, 3, 4, 5, and 6 correspond to oscillation periods of 8, 16, 32 and 64 days, respectively. We superimpose a cumulative coherence plot on the gray-scale images. The bars indicate our "detection level" for stacked coherence, estimated to be at least the 98% confidence level for nonrandomness.

Germany, 49.8°N 7°E), shown in Figure 2. Here we see that decreases in cloud cover typically correlate with increases in sulfate surface concentration. Such cloud "dips" can persist for extensive periods, such as from days 320–350. Peaks in deposition flux generally cluster together in time periods with low sulfate air concentrations. It is not uncommon for such clusters to persist for 10–20 days. Thus we see that the sulfate concentration rises during relatively clear periods (when clouds do not inhibit gas-phase production) and decreases during cloudy, rainy periods (when precipitating clouds scavenge sulfate and/or clouds inhibit gas-phase sulfate production). In the next section we apply statistical approaches to quantify such relationships in the data series.

3. Statistical Methods

[10] For estimating the correlation between cloud cover and sulfate concentration, deposition or precipitation, we apply time series algorithms that use Slepian wavelets [*Lilly and Park*, 1995; *Bear and Pavlis*, 1999; *Park and Mann*, 2000]. We use wavelets instead of standard Fourier transforms to account for possible nonstationary behavior in the data correlations. For instance, if aqueous sulfate-production and cloud-scavenging dominate in different time intervals, a wavelet-based correlation estimate can detect competing episodes of strong correlation that are sometimes positive, and sometimes negative. Correlation estimates based on the Fourier-transform tend to average behavior over entire time series, and can appear weak if the correlation phase varies with time.

[11] Slepian wavelets are designed as the counterparts of Slepian tapers, which are used in multiple taper spectrum analysis [*Thomson*, 1982; *Park et al.*, 1987a, 1987b; *Percival and Walden*, 1993]. In particular, Slepian wavelets are derived from an optimization condition that, for a spectrum estimate at frequency f_o, minimizes spectral leakage outside a specified frequency interval $[f_o - f_w, f_o + f_w]$. The leakage-resistance condition takes the form of an eigenvector problem. Its solution is a sequence of wavelets that (1) possess optimal spectral leakage properties (2) have either odd or even parity, and (3) are mutually orthogonal. Even and odd wavelets can be paired as real and imaginary parts of a complex-valued wavelet, in order to constrain the phase of a signal. Mutual orthogonality affords statistical

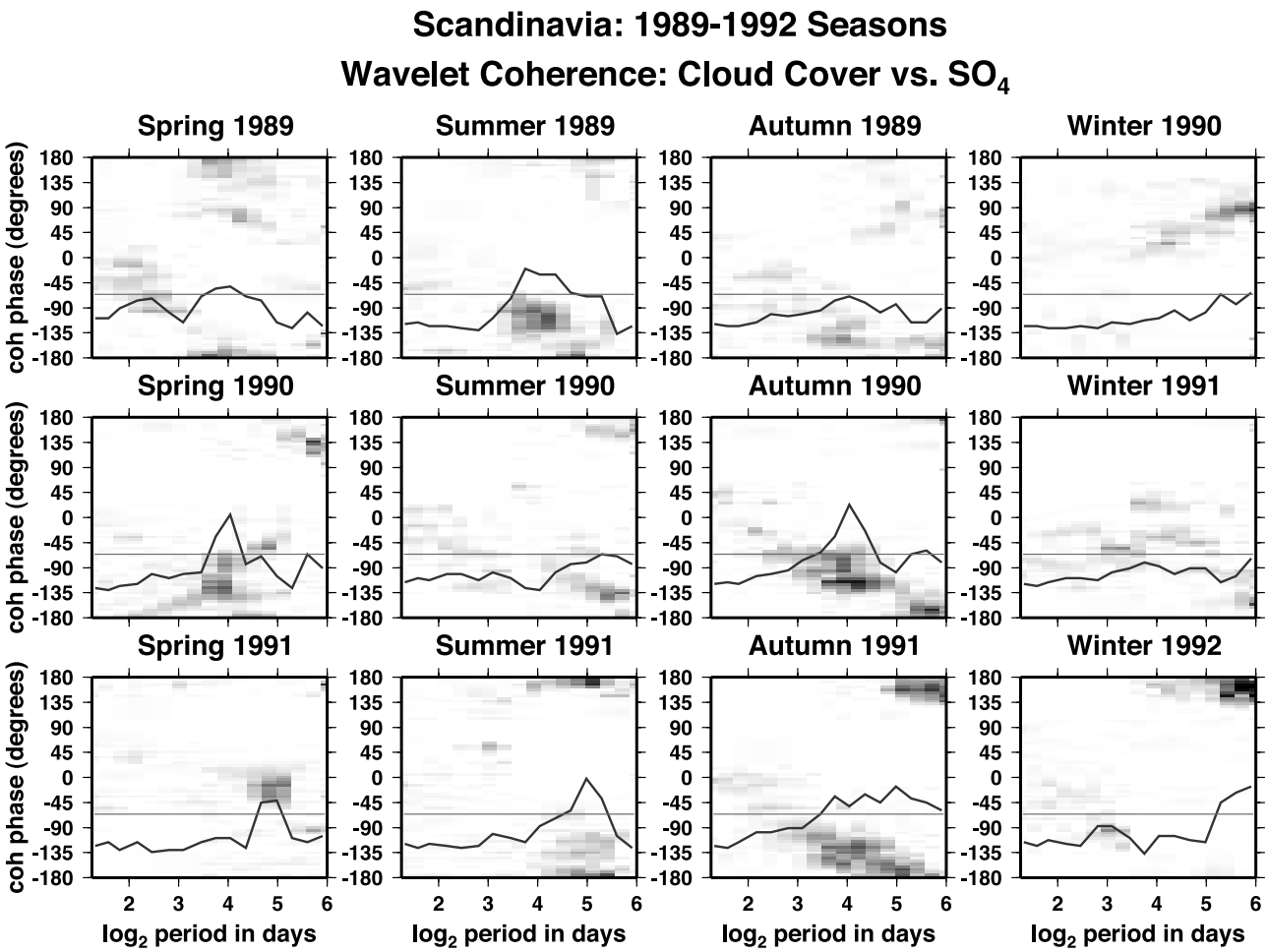

Figure 4. Same as Figure 3 but for Scandinavia. On the log-period axis, 3, 4, 5, and 6 correspond to oscillation periods of 8, 16, 32 and 64 days, respectively.

independence among wavelet transforms computed with different wavelet pairs.

[12] We compute the phased wavelet transform of time series of observations or GCM model output (described below) at a collection of cycle periods $T_k = 1/f_k$, where f_k are a set of logarithmically spaced frequencies. We use three complex-valued Slepian tapers with time-bandwidth $p = 2.5$ [*Lilly and Park*, 1995] and compute coherence $\mathcal{C}$ between time series at matching points in time and frequency. The phase ϕ of the coherence $\mathcal{C}$ translates into the time delay or sense of correlation: $\phi \approx 0^\circ$ is positive correlation, $\phi \approx \pm 180^\circ$ is negative correlation. Note that the phase angle

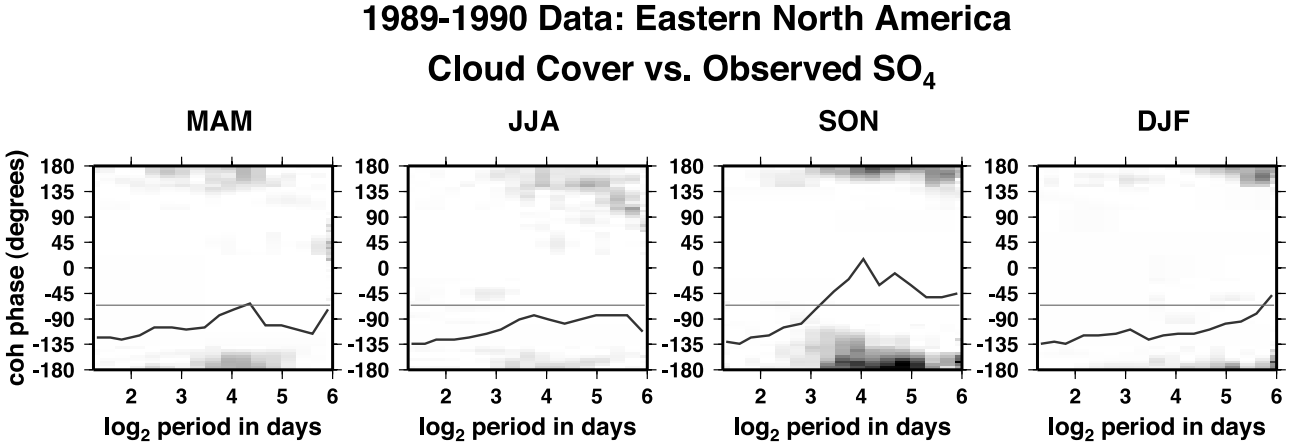

Figure 5. Same as Figure 3 but for North American stations, shown for 1989–1990. On the log-period axis, 3, 4, 5, and 6 correspond to oscillation periods of 8, 16, 32 and 64 days, respectively.

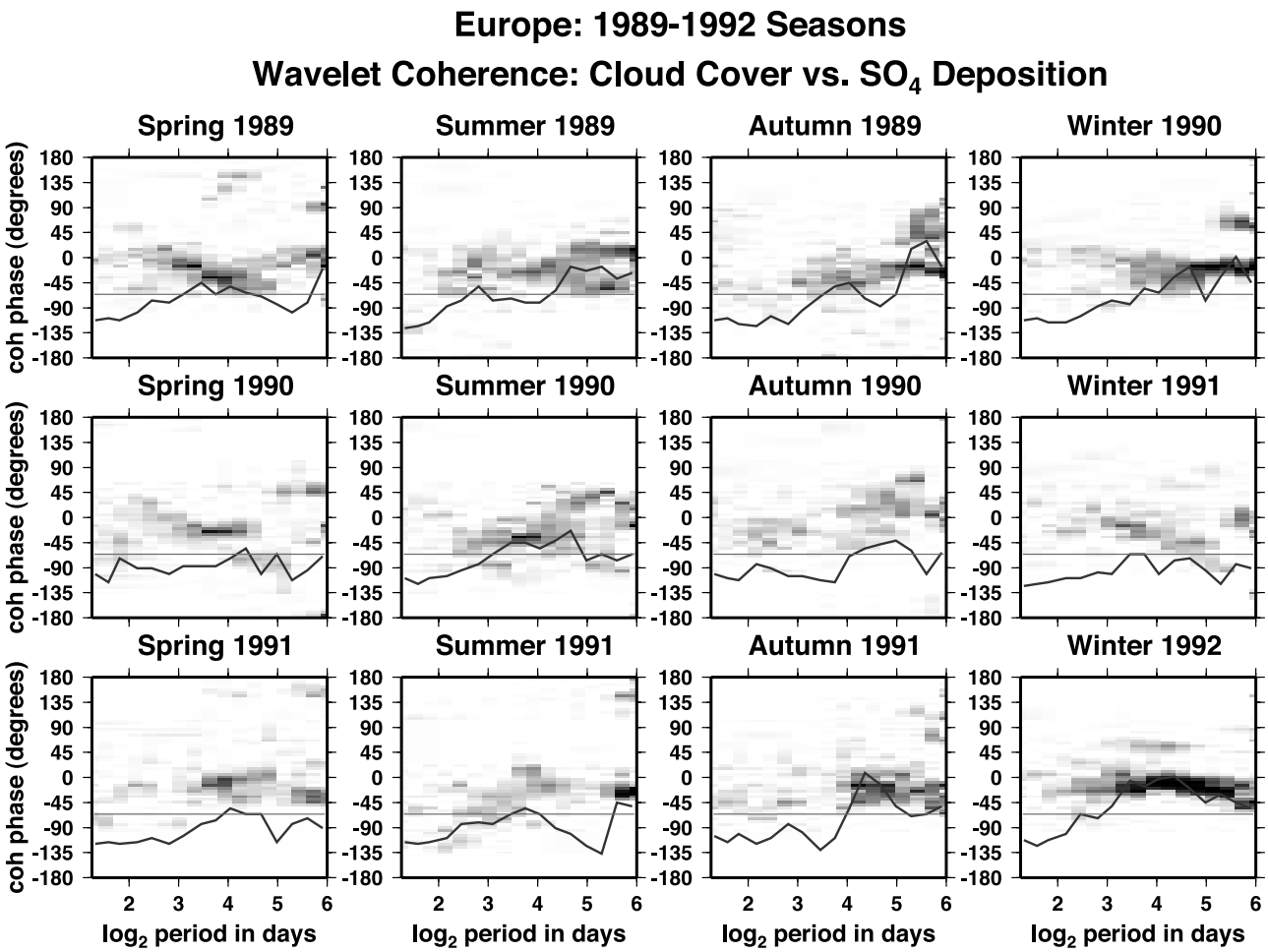

Figure 6. Squared coherence between cloud cover and sulfate deposition for Europe. On the log-period axis, 3, 4, 5, and 6 correspond to oscillation periods of 8, 16, 32 and 64 days, respectively.

"wraps around" every 360°, so that two values of coherence $\mathcal{C}$ with phases $\phi = 179°$ and $\phi = -179°$ differ by only 2°.

[13] Other phase relationships include fixed time delays and derivative relationships. For instance, if a time series $\{X_t\}_{t=1}^N$ is delayed 4 days relative to time series $\{Y_t\}_{t=1}^N$, the coherence of X_t relative to Y_t will have phase $\phi = -180°$ at T = 8-day cycle period, $\phi = -90°$ at T = 16-day cycle period, and $\phi = -45°$ at T = 32-day cycle period. Alternatively, if $\{X_t\}_{t=1}^N$ is correlated with the rate-of-change, or time derivative, of $\{Y_t\}_{t=1}^N$, then the coherence of X_t relative to Y_t will have phase $\phi = 90°$ over a broad range of cycle periods. Derivative relationships have practical applications. If clouds influence aqueous-phase sulfate production and little else, and there is a steady supply of SO_2 to oxidize, we would expect cloud-sulfate coherence $\mathcal{C}$ with $\phi = 90°$.

[14] The squared coherence $\mathcal{C}^2$ can be related to confidence levels for nonrandomness using standard statistical assumptions. For a correlation using 3 complex-valued Slepian wavelets, $\mathcal{C}^2$ values can be compared to an F variance ratio with 2 and 4 degrees of freedom. A stacked coherence of time series from M stations or M GCM grid points can be compared to the confidence limits of an F variance ratio with $2M$ and $4M$ degrees of freedom.

[15] In any time interval of interest (e.g., month, season or year), we plot wavelet coherence as a gray-scale intensity versus log-period (days) and phase delay in degrees. This scheme allows the concentration of coherence at a particular phase or phases to be expressed visually (e.g., Figure 2). We superimpose a plot of cumulative coherence on the gray-scale images, in which $\mathcal{C}^2(f)$ is summed over phase bins in 120° intervals. We sum over restricted phase intervals, rather than summing all phases from −180° to 180°, because we seek to detect simple causal relationships between clouds and atmospheric sulfate. Correlations with highly variable phase would, practically speaking, be much harder to interpret. We plot the cumulative coherence, as a function of log-period, against a detection threshold that we specify below.

[16] The "detection line" for cumulative coherence $\mathcal{C}^2(f)$ is the nominal 99% confidence limit for nonrandomness for the following joint probability: that the coherent fraction of the signal is both sufficiently large and also concentrated in a 120° phase interval. We compute the confidence limit for the stacked coherence of $M = 10$ independent time series, computed with separate terms corresponding to whether 1, 2, 3, ... or 10 coherence estimates lie in the same 1/3 of the phase circle. The statistics are a hybrid of the F variance ratio

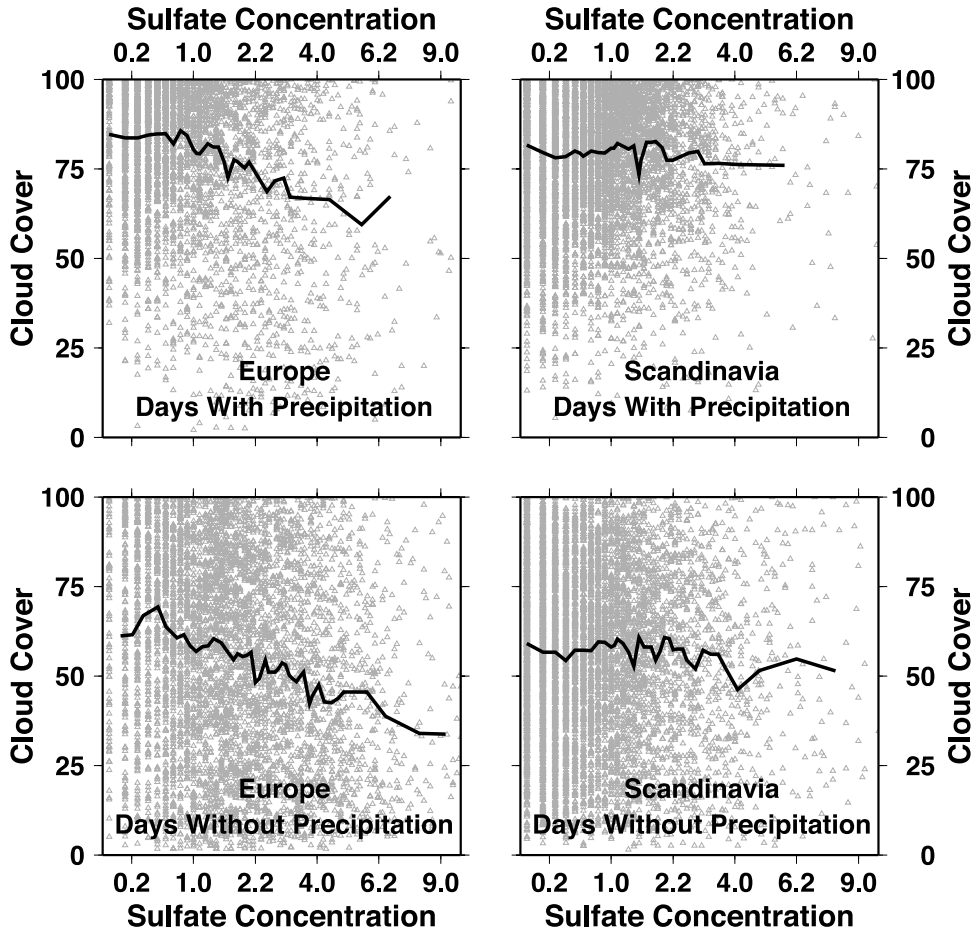

Figure 7. Scatterplot of cloud cover versus(log) sulfate concentration (μg S m^{-3}) for Europe and Scandinavia, distinguishing between days with (top) and without (bottom) precipitation. Superposed is a curve showing the median.

and binomial counting probabilities, and specifies stacked-$C^2 = 0.321$ as the 99% confidence level for nonrandomness. Because we typically stack coherences from $M > 10$ time series, this confidence limit is slightly conservative. However, we plot the largest stacked coherence among a selection of 120° phase intervals, so the actual confidence limit of our "detection line" is lower than 99%. Numerical tests suggest the $C^2 = 0.321$ detection level represents roughly 98% confidence for nonrandomness.

4. Observation Results

[17] We show results of coherence between cloud cover and sulfate concentration for the aggregate of the 11 European stations (those south of 52.3°N) in Figure 3. The coherence phase, as a function of period, is shown for each season. For every season observed there is coherence at >98% confidence level for some range of cycle periods. This coherence has phase near ±180°, meaning that clouds and sulfate are anticorrelated. The oscillatory periods that exhibit anticorrelation are large but variable, ranging from 8–64 days. Note that a given period includes both a peak and a trough, so that an 8 day period would consist of 4 days of peak sulfate/reduced cloud cover and 4 days of low sulfate/peaked cloud cover. There is a slight preference for coherence phases in the range −135° to −180°, which indicates a tendency for cycle-maxima in sulfate (and minima) to suffer a slight delay relative to cycle-minima in cloud cover (and maxima).

[18] Coherence is not as strong or as consistent for Scandinavia, represented by the 10 sites to the north of 52°N (Figure 4), but does exceed the 98% confidence level in 8 of the 12 seasons. In some seasons there is a trend from positive correlation at shorter periods (4–8 days) to negative correlation at longer periods (e.g., in summer 1989, autumn 1990 and autumn 1991). These trends are consistent with anticorrelation with a 2–4-day delay in the sulfate cycle, relative to cloud cover. Alternatively, peaks in aggregate coherence near T = 16-day cycle period and $\phi = -90°$ for summer 1989, spring 1990, and autumn 1990, could be interpreted as a negative correlation between clouds and the first derivative of sulfate, that is, a correlation between clouds and sulfate removal. Weak positive correlation between clouds and sulfate is evident intermittently at short period in Figure 4, and may result from low-level nonprecipitating clouds which are more prevalent at high latitudes; these clouds would generate sulfate but not scavenge it. This is speculative, however, since aggregate positive coherence at short period does not exceed the 98% confidence level in any season.

Table 1. Global Annual Sulfur Budgets

	Standard	Chem	CLD Budget
	SO2		
Sources, Tg S yr^{-1}			
Emissions	70.8	70.8	70.8
Photochem	9.9	9.9	9.9
Sinks, Tg S/yr			
Dry deposition	−34.8	−35.5	−34.7
Wet deposition	−1.0	−1.0	−1.0
Gas phase	−13.1	−11.6	−11.3
Aqueous phase	−31.7	−32.6	−33.6
Burden, Tg S	0.63	0.66	0.64
Lifetime, days	2.9	3.0	2.9
	Total Sulfate		
Sources, Tg S yr^{-1}			
Industrial emissions	1.9	1.9	1.9
Gas phase	13.1	11.6	11.3
Aqueous phase	31.7	32.6	33.6
Sinks, Tg S yr^{-1}			
Dry deposition	−5.7	−5.8	−3.2
Wet deposition	−41.1	−40.4	−43.7
Burden, Tg S	0.72	0.71	0.54
Lifetime, days	5.6	5.6	4.2
	Sulfate From Gas-Phase Production		
Sources, Tg S yr^{-1}			
Gas phase	13.1	11.6	11.3
Sinks, Tg S yr^{-1}			
Dry deposition	−0.4	−0.4	−0.3
Wet deposition	−12.8	−11.2	−11.0
Burden, Tg S	0.41	0.39	0.36
Lifetime, days	11.3	12.2	11.7
	Sulfate From Aqueous-Phase Production		
Sources, Tg S yr^{-1}			
Industrial emissions[a]	1.9	1.9	1.9
Aqueous phase	31.7	32.6	33.6
Sinks, Tg S yr^{-1}			
Dry deposition	−5.3	−5.4	−2.9
Wet deposition	−28.3	−29.2	−32.7
Burden, Tg S	0.31	0.32	0.17
Lifetime, days	3.4	3.4	1.7

[a]The particulate sulfate emission is arbitrarily added to the aqueous emission.

[19] The coherences from the North American data (Figure 5) exhibit negative correlation at 8–64-day period for most of the year, with greatest statistical significance in fall 1989.

[20] The anticorrelation between clouds and sulfate is due at least in part to the precipitation scavenging of sulfate. Figure 6 shows coherence between cloud cover and sulfate in precipitation (deposition) at the European stations. Significant positive correlation is observed for most of the seasons, again typically at cycle periods of 8–64 days. Coherence between clouds and precipitation (not shown) looks very similar to Figure 6. Indeed, coherence between precipitation and sulfate deposition (also not shown) is very strongly significant and positive at all timescales. One would expect this because precipitation always results in some amount of sulfate deposition.

[21] We use the precipitation information to distinguish between days when scavenging was active and days when clouds were present but not depleting sulfate. By looking only at days without precipitation, a positive correlation between cloud cover and sulfate would show evidence of cloud production. By dividing our data into days with and without precipitation, we fragment our continuous time series and cannot estimate coherence as a function of cycle period. However we may examine scatterplots of cloud cover and sulfate air concentration to see whether days with higher cloud cover correspond to days with more sulfate (i.e., aqueous-phase sulfate production). There is considerable scatter in the daily data (Figure 7), so we compute a running estimate of the median cloud cover in narrow intervals of sulfate concentration. Median cloud cover in Europe decreases with increasing sulfate concentration, whether the clouds are precipitating or not. In Scandinavia there is no trend in the median cloud cover for either type of cloud. It is possible that an analysis sensitive to the presence of thick tall clouds with high liquid water content might reveal a positive trend, since such clouds may generate more sulfate. However our analysis, which is most sensitive to thin, aerially extensive clouds, detects no increase in sulfate with cloud cover.

[22] We find that in general, sulfate and clouds are negatively correlated. In the data sets we examine, coherence is most significant in Europe. The negative correlation indicates that when clouds are prevalent, sulfate is not, and vice versa; and that therefore clouds may (1) play a greater role in scavenging sulfate than producing it, and/or (2) may inhibit, rather than enhance, the main oxidation pathway for sulfate production in the atmosphere. A slight bias in coherence phases between −90° and −180° supports this interpretation, as it indicates that positive (negative) fluctuations in cloud cover tend to precede negative (positive)

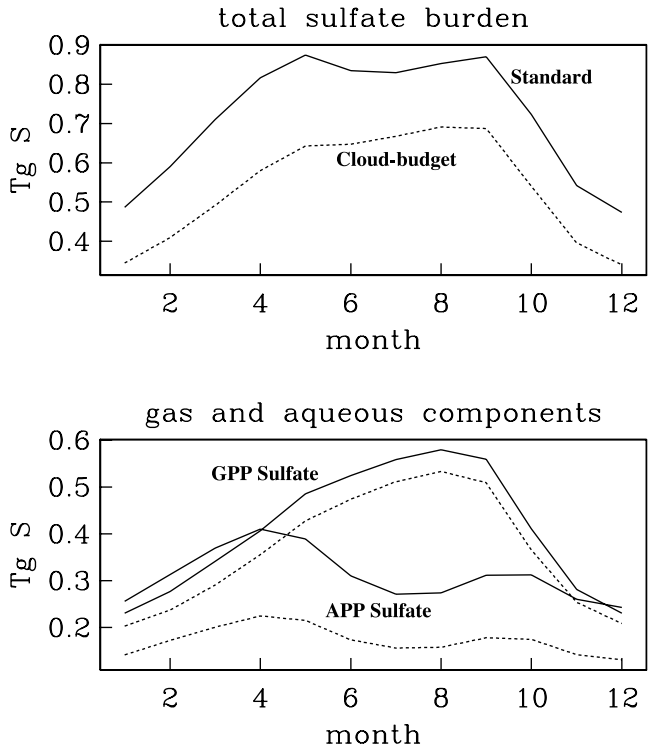

Figure 8. Model sulfate burden as a function of month for the standard run (solid) and the cloud chemistry budget run (dashed). Upper is total sulfate, lower shows the aqueous and gas-phase components.

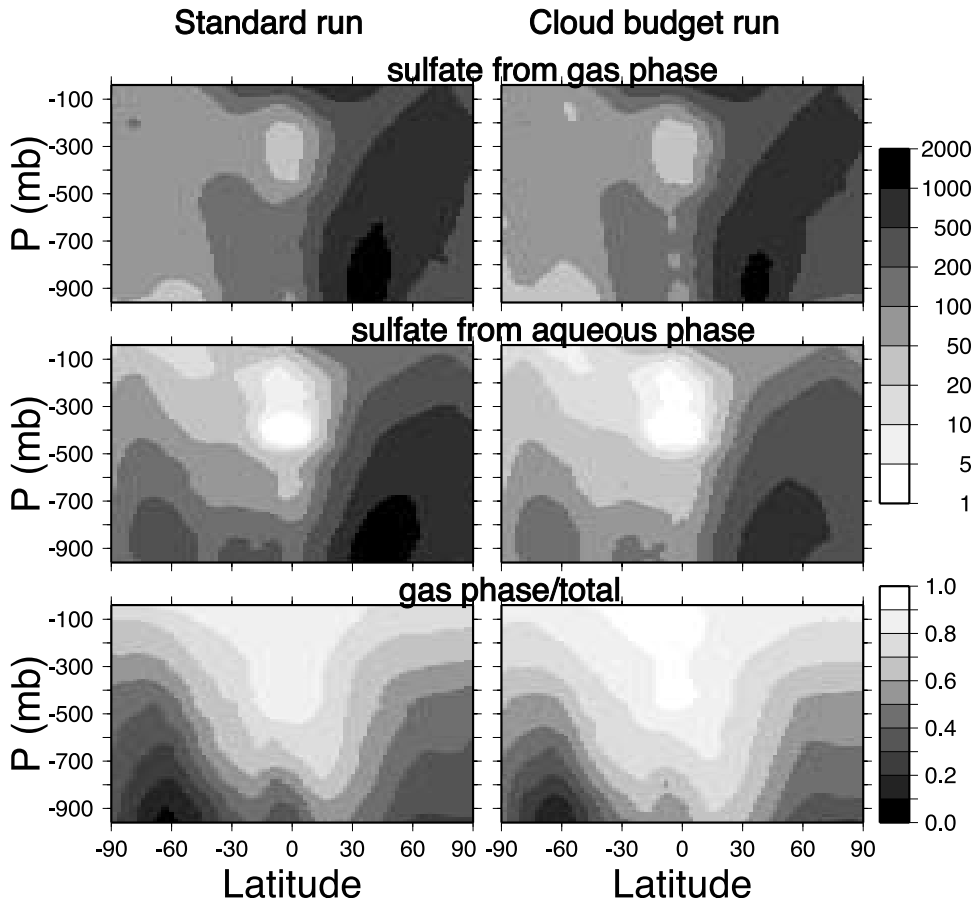

Figure 9. Zonal annual mean of the gas-phase produced sulfate, aqueous-produced sulfate, and gas-phase divided by the total sulfate for the standard run (1st column) and the cloud budget run (2nd column). The concentrations unit is ng m^{-3}. See color version of this figure at back of this issue.

fluctuations in sulfate. That is, clouds tend to build up before precipitating and scavenging sulfate, and/or gas phase produced (GPP) sulfate builds up following cloud dissipation.

[23] In the following section we will consider cloud-sulfate coherence in our global model. We will use the model to consider the relative contributions of gas and aqueous sulfate production pathways to the correlation behavior.

5. Model Experiments

[24] We perform 3 model simulations, using the Goddard Institute for Space Studies General Circulation Model (GISS GCM), with online sulfur chemistry. This version of the model is described by *Koch et al.* [1999]. The model has resolution of $4^\circ \times 5^\circ$ and 9 vertical layers. Online species include DMS, SO_2, gas phase produced (GPP) sulfate, aqueous phase produced (APP) sulfate and H_2O_2. Since we are interested in distinguishing between aqueous (in-cloud) phase and gas-phase sources of sulfate, we have made these separate species.

[25] The aqueous sulfur chemistry is embedded in the cloud code, so that dissolution and sulfate production occur after cloud condensation, the soluble species are scavenged with autoconversion, they are returned to the grid box following evaporation, and they are transported along with air mass flux (e.g., in convective updrafts and downdrafts). Beneath precipitating clouds, gases and aerosols are scavenged by falling raindrops; sulfate production may also occur within these droplets. (In these simulations we do not include a sulfate indirect effect.) Aqueous-phase sulfate production is achieved by oxidation of SO_2 with H_2O_2. We use a semiprognostic treatment of H_2O_2, using off-line HO_2, OH and photolysis rate to generate and destroy H_2O_2. This allows the oxidant to have a budget that may be depleted by sulfate generation and cloud processing. Gas-phase sulfate production occurs by oxidation of SO_2 with (off-line) OH.

[26] The emissions include anthropogenic fossil fuel and biomass burning SO_2, natural DMS and steady volcanic SO_2 [see *Koch et al.*, 1999]. For the coherence calculations, we save daily average sulfate surface concentrations and cloud cover at each grid box shown in the hatched regions of Figure 1.

6. Standard Model

[27] Our initial simulation is identical to the simulation described by *Koch et al.* [1999], except that we carry separate GPP and APP sulfate species. It is of interest to compare the budgets of these 2 pathways, shown in the first column of Table 1. Although most of the sulfate is generated in the aqueous phase (about 70%), this component is

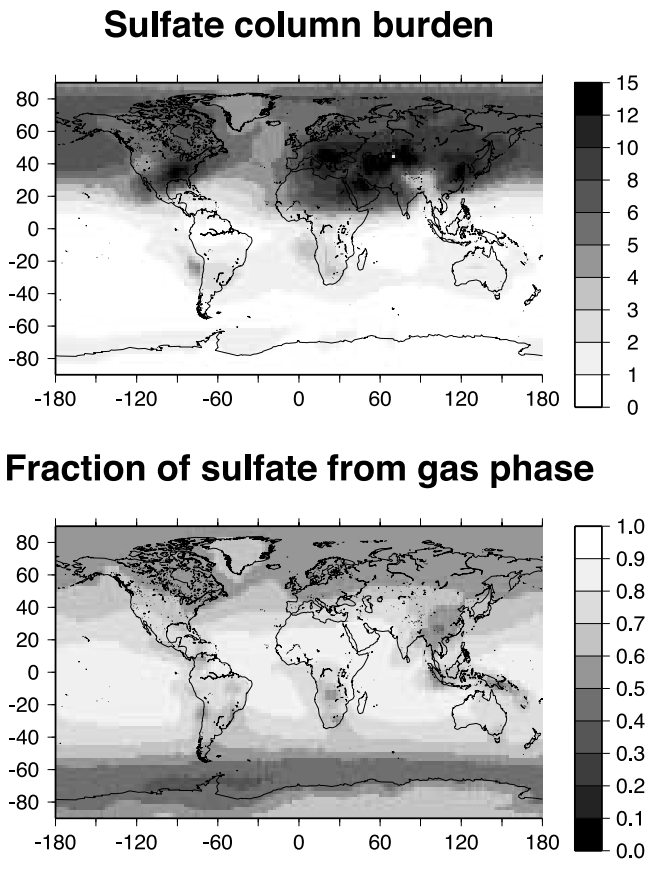

Figure 10. Annual average column burden of (total) sulfate (mg m^{-2}) at top. Below is the fraction derived from gas-phase production. See color version of this figure at back of this issue.

more efficiently scavenged by the local clouds, so it has a relatively short lifetime (3.4d on global average) and makes up only about 43% of total burden. Conversely, the gas-phase-produced (GPP) sulfate is about 30% of the total source, but since it is produced in relatively clear conditions, it persists longer (11.3d) and makes up 57% of the total burden. *Barth et al.* [2000] also distinguished between the sulfate oxidation pathways; their result is similar, however they had higher aqueous-phase production (81%) and contribution to burden (50–60%).

[28] Figure 8 shows how the sulfate burden and its 2 components vary during the year. The gas-phase contribution is greatest in April–October, when there is the most sunlight in the NH where the (industrial) emissions are greatest.

[29] Figure 9 shows the zonal annual mean sulfate produced in the gas phase, aqueous phase and the ratio of the GPP sulfate over the total. Gas-phase production is dominant at high altitudes and where convective scavenging efficiently removes sulfate made in-cloud (i.e., in the tropical upper troposphere). Figure 10 shows the geographic distribution of the column burden of sulfate and the fraction of the column burden derived from gas-phase production. There is some tendency for aqueous-phase production to be higher over continents (near source regions) since this pathway is faster than gas-phase oxidation.

[30] We performed a coherence analysis of model sulfate and cloud cover, saving diagnostics in the 3 regions of Figure 1 in a manner like the observations: 24-hour averages of cloud cover and sulfate concentration in the lowest model layer. Following a 1-yr model spin-up we saved daily diagnostics for 3 years. The coherence of total sulfate and cloud cover in Europe is shown in Figure 11. There is some significant anticorrelation (e.g., in the spring and fall of the first year, in the winter and fall of the second year), but not nearly as strong or as negative as observed (Figure 3). In Figure 12 we show the coherence between clouds and the GPP sulfate only. We see that without the aqueous-phase-produced (APP) sulfate, the correlation is stronger and more negative, closer to the observed correlations.

[31] We show model results from Europe only. In Scandinavia and North America the modeled coherence is weaker than in Europe. The correlation between total sulfate and cloud cover is more positive (than in Europe); as in Europe, the correlation becomes more negative if GPP sulfate is considered in isolation.

7. Potential Impact of Missing Photochemical Effects

[32] One reason our coherence is too weak in the model may result from the importing of monthly mean oxidants from another model, so that the OH and therefore the gas-phase sulfate production do not increase under clear conditions and decrease under cloudy conditions. If our aerosol model were fully coupled to a chemistry model then the gas-phase source of sulfate would diminish beneath a cloud and presumably generate some negative correlation between the two.

[33] To test this, we repeated the simulation, setting gas-phase production of sulfate equal to zero if a cloud is overhead (“chem run”). Figure 13 shows that this does strengthen the negative correlation between cloud cover and GPP sulfate for Europe (compared with Figure 12). Moreover, the GPP-only coherence exhibits a bias toward phases ϕ in the range $-135°$ to $-180°$, similar to the Europe data. However there is very little change in the coherence between clouds and total sulfate (not shown), since the in-cloud production is dominant.

[34] The global budget for this simulation is shown in the middle column of Table 1. There is little change compared with the control run.

[35] These first 2 experiments give us a clue that perhaps gas-phase production should be more important relative to aqueous-phase production, since the GPP sulfate has the desired negative correlation but adding the APP sulfate “washes out” the signal.

8. Addition of Dissolved Tracer Budget

[36] Another aspect of the model that has an impact on the sulfate-cloud relations is the treatment of dissolution and aqueous sulfate production. Sulfate generated within a cloud should either rain out of the cloud or be released from the cloud when the cloud evaporates. This model, like other global sulfur models, releases its APP sulfate from the cloud following each (cloud) time step whether the cloud evapo-

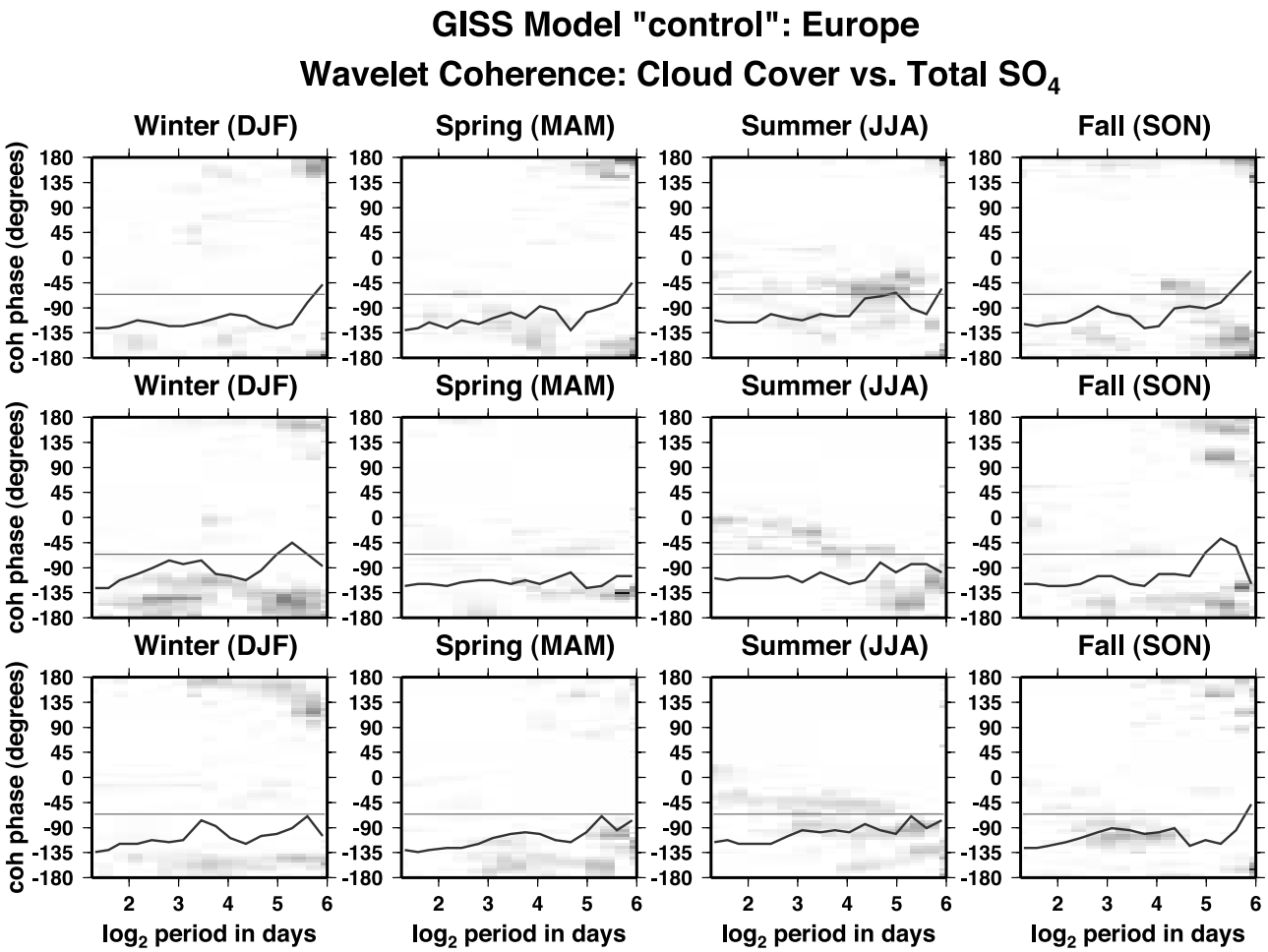

Figure 11. Coherence of modeled total sulfate and cloud cover in Europe, plotted for each season of 3 years. See Figure 3 for details. On the log-period axis, 3, 4, 5, and 6 correspond to oscillation periods of 8, 16, 32 and 64 days, respectively. The bars indicate our "detection level" for stacked coherence, estimated to be at least the 98% confidence level for nonrandomness.

rates or not. This allows some of the sulfate to escape into the cloud-free region of the box instead of remaining in the cloud where it more likely to be rained out.

[37] To correct this, we repeated the ("chem") simulation, this time retaining APP sulfate for the duration of the cloud lifetime and releasing it into the cloudless portion of the box only if the cloud evaporates. As a result, the APP sulfate, now trapped in the cloud droplets, is more likely to be scavenged. As shown in Table 1 (column 3), this causes the APP burden and lifetime to drop to about 1/2 of their values in the standard simulation; the total sulfate burden drops by 25%. The decrease in the APP sulfate occurs throughout the troposphere (Figure 9) and, conversely, the increase in fractional amount of GPP sulfate occurs throughout the troposphere (comparing the bottom 2 panels). Figure 8 shows that the reduction in APP sulfate occurs throughout the year.

[38] Figure 14 shows that this simulation produces significant negative coherence between cloud cover and total sulfate over Europe for most of the seasons simulated, much more than in the standard simulation (Figure 11). The improvement was similar in North America, but less in Scandinavia (where the APP sulfate is perhaps still too dominating). The cycle period of coherence is long, as in the observations.

[39] Since the coherence in this simulation was most like the observations, we performed further GCM simulations to investigate the timescale and vertical extent of the cloud impact on sulfate. To test whether coherence at shorter timescales would appear if our time series was saved at smaller time steps, we saved hourly diagnostics; there was still no significant short period coherence. We also saved (for one year) the daily total sulfate produced and scavenged by the clouds, in order to compare with the observations and to see if a shorter timescale correlation appeared. These coherences are shown (for Europe) in Figure 15. The correlations for both are significant and positive. The coherence between clouds and sulfate deposition is stronger in the model than the observations (Figure 6) and is significant at shorter periods than observed, though the most significant correlation is at the longer periods. The stronger model coherence may be due to the tendency for the model clouds to drizzle more frequently than observed. Similar to the total sulfate, daily sulfate produced in clouds

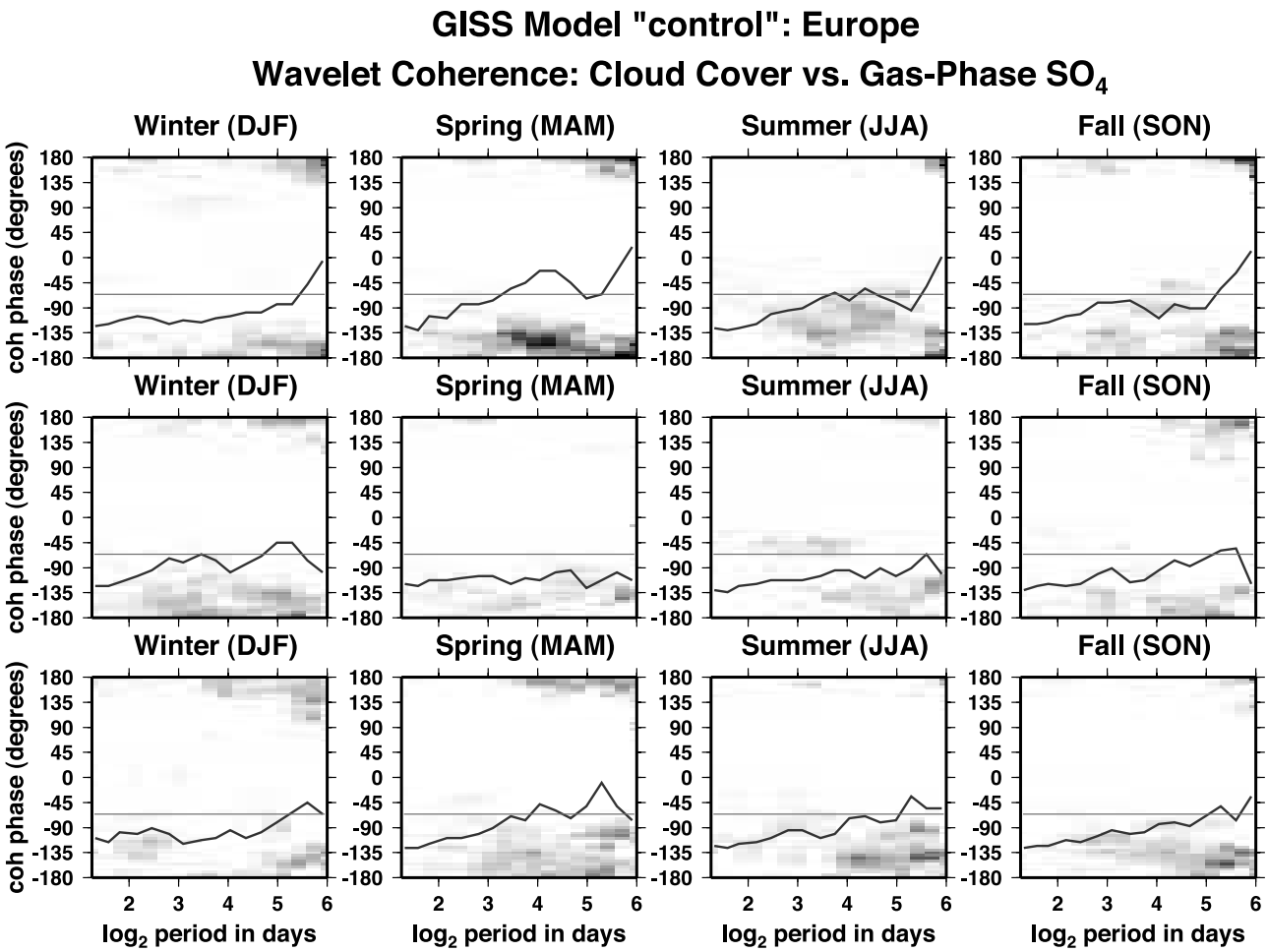

Figure 12. As in Figure 11 but for sulfate from gas-phase production only.

correlates with clouds on a relatively long timescale. We will continue the discussion of timescale in the following section.

[40] Finally, we tested whether layer 1 sulfate concentrations are representative of the sulfate at higher levels in the model, where the clouds typically reside. To investigate this we saved the sulfate in layers 1, 2, 3 and 4 (layer 4 is at 635 mbar) for one model year. We found a very strong positive coherence between layers 1 and layers 2–4. Also the coherence between clouds and layers 2 and 3 is very similar to the coherence with layer 1 although it is not quite as strong. The slightly stronger coherence with layer 1 may result from the effects of below cloud scavenging and/or inhibition of gas-phase sulfate production below clouds, which would be greatest in the lowest layer.

[41] Although the model coherence (Figure 14) is now similar to the observed coherence (Figure 3), it is still not as strong. In the following section we consider some further possible means to strengthen the model coherence.

9. Discussion and Conclusions

[42] We have examined 3 years of daily (ISCCP) cloud cover and sulfate surface concentration observations and shown that these have a persistent negative correlation in Europe and North America. This result suggests that clouds inhibit sulfate production more than they enhance it via in-cloud production. The inhibition results from a combination of precipitation scavenging of sulfate and the reduction of gas-phase production (GPP) below clouds. Our model simulation indicated that negative correlation is characteristic of cloud-GPP sulfate relations. Indeed the model simulations improved (i.e., showed greater anticorrelation between clouds and sulfate) when we made changes that decreased in-cloud production relative to gas-phase production.

[43] We attempted to seek evidence of in-cloud sulfate production in the data by looking for a positive trend between sulfate amount and cloud cover in clouds that are nonprecipitating. Such a trend was either lacking or negative, depending upon the region. Thus we saw little evidence of in-cloud production and conclude that its role is minor compared with the other cloud influences on sulfate. We note however that our analysis may not be best suited for detecting APP sulfate. This is because the most APP sulfate may be generated by clouds which are thick, columnar and having high cloud liquid water content and since these are generally less aerially extensive they may not be associated with large cloud cover. Our analysis is more sensitive to thinner, less productive but aerially extensive clouds.

[44] The timescales of coherence were fairly long, typically 8–64 days. These timescales appeared also in coher-

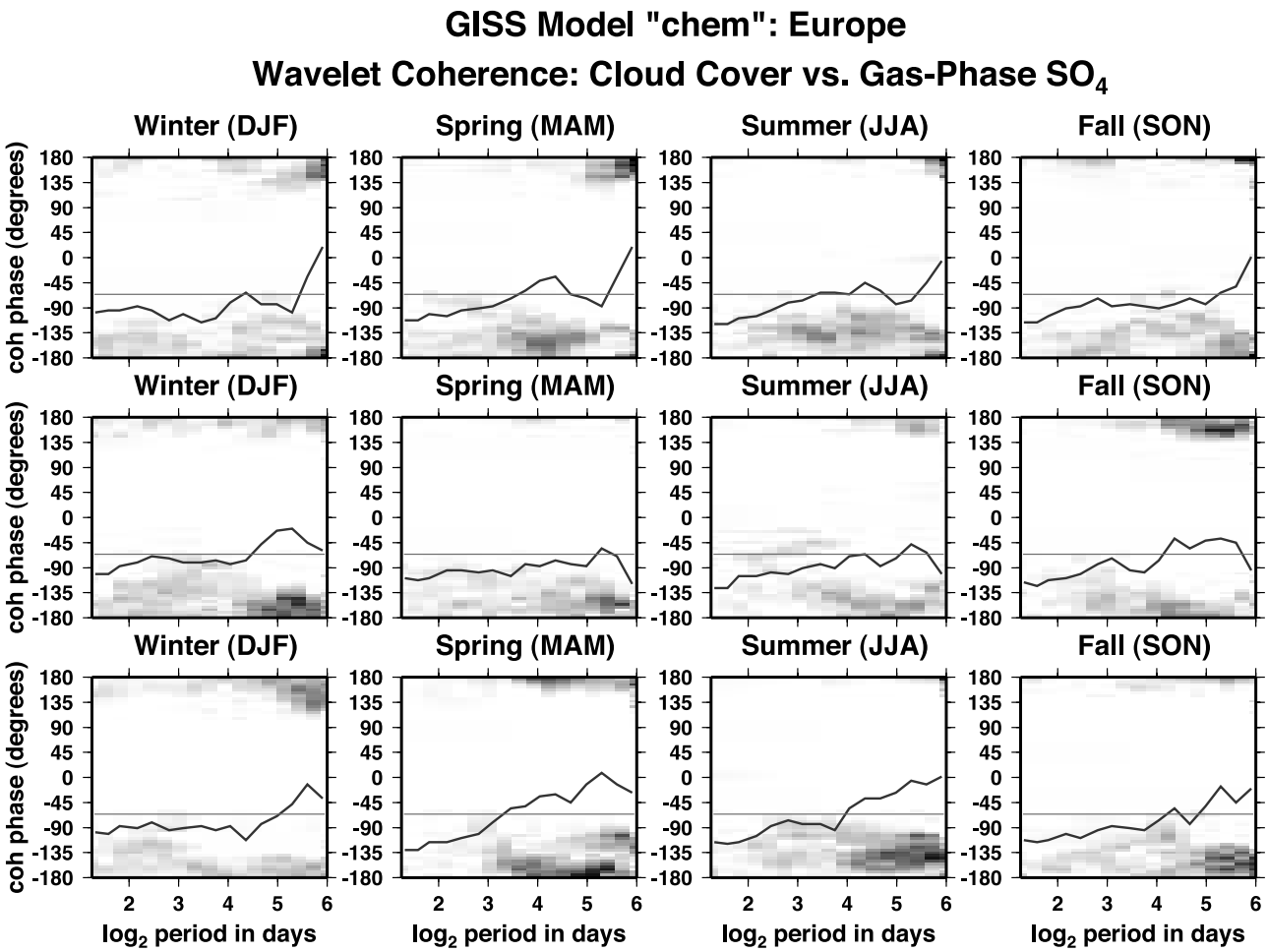

Figure 13. As in Figure 11 but for sulfate from gas-phase production only for the simulation without gas-phase production under clouds.

ence between cloud cover and sulfate deposition. The long timescales probably result from the fact that the sulfate concentration in a given location is influenced by the integration of cloud effects over a broad surrounding region, which translates into a lengthening of timescale. Furthermore, the sulfate responds to the cloud systems which in turn are influenced by various intramonthly modes (e.g., blocking episodes, index cycle, regional midlatitude wave trains; *Lanzante* [1990]; *Schubert* [1985]). While a given sulfate particle has a relatively short lifetime (on the scale of days to a few weeks), the sulfate concentration level is maintained or depleted by the ongoing production and removal mechanisms, many of which are cloud-related. The slow shifting from cloudy to clear conditions and the responses of the sulfate concentration and deposition are illustrated in the sample time series shown in Figure 2. Finer time-scale correlations (including evidence of in-cloud production) might appear if one were to observe sulfate in and around a single cloud over the course of its lifetime. On the larger time and spatial scales of our observations, however, only anticorrelation is preserved.

[45] Our regions of study, those with daily sulfate surface concentration measurements, were primarily located near large anthropogenic source regions. The anticorrelation result was strongest in Europe, where we also had the most data. In Scandinavia and in the U.S., the coherence was weaker. In Scandinavia this may be a combination of higher in-cloud production and lower gas-phase production (due to the higher latitude). Since the North American data set is only for one year it is difficult to speculate about "typical" behavior there. In other regions, more remote from anthropogenic sources, the correlation behavior could be different. We attempted to look at data from some oceanic stations (e.g., Izana, Bermuda, Barbados; J. Prospero, private communication, 1997), however the data were too sparse to get a significant result.

[46] We were able to use the observations to improve our global sulfur model. Initially the model produced little significant coherence between sulfate and cloud cover. We improved it by adding a dissolved sulfate budget, so that sulfate generated within a cloud is not released from the cloud unless the cloud evaporates. Hence more sulfate is rained out and less generated by clouds. The overall sulfate burden and lifetime are reduced by 25% (to 0.54 Tg S and 4.2d, respectively). This burden is at the low end of other global sulfate simulations (which range from about 0.50–0.95 Tg S). The lack of a dissolved species budget is typical of global aerosol models. Thus we expect that other global sulfate models would fail to generate the negative correlations between clouds and sulfate which appear in the

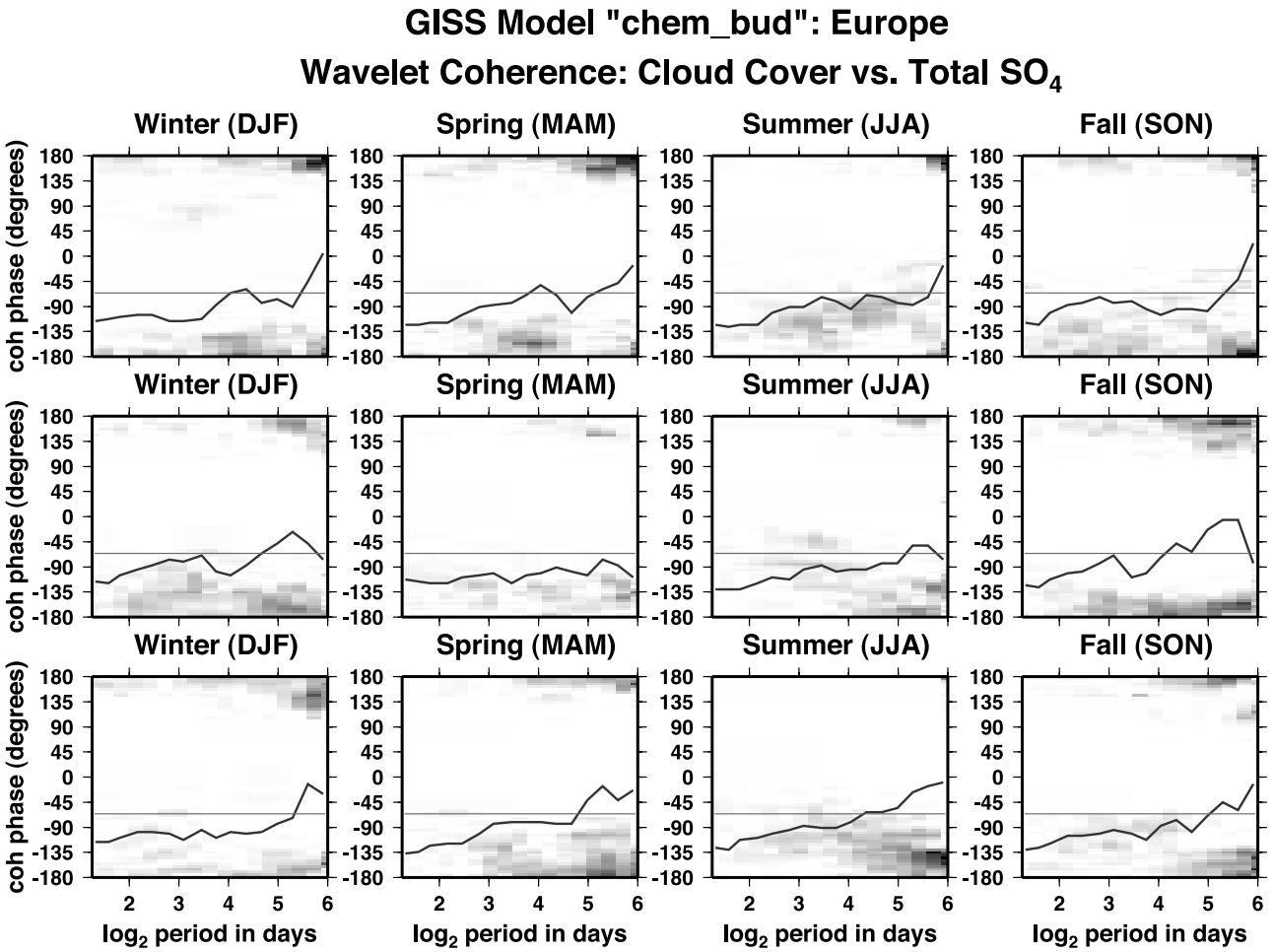

Figure 14. As in Figure 11 from the simulation with no gas phase production beneath clouds and including a dissolved sulfate budget.

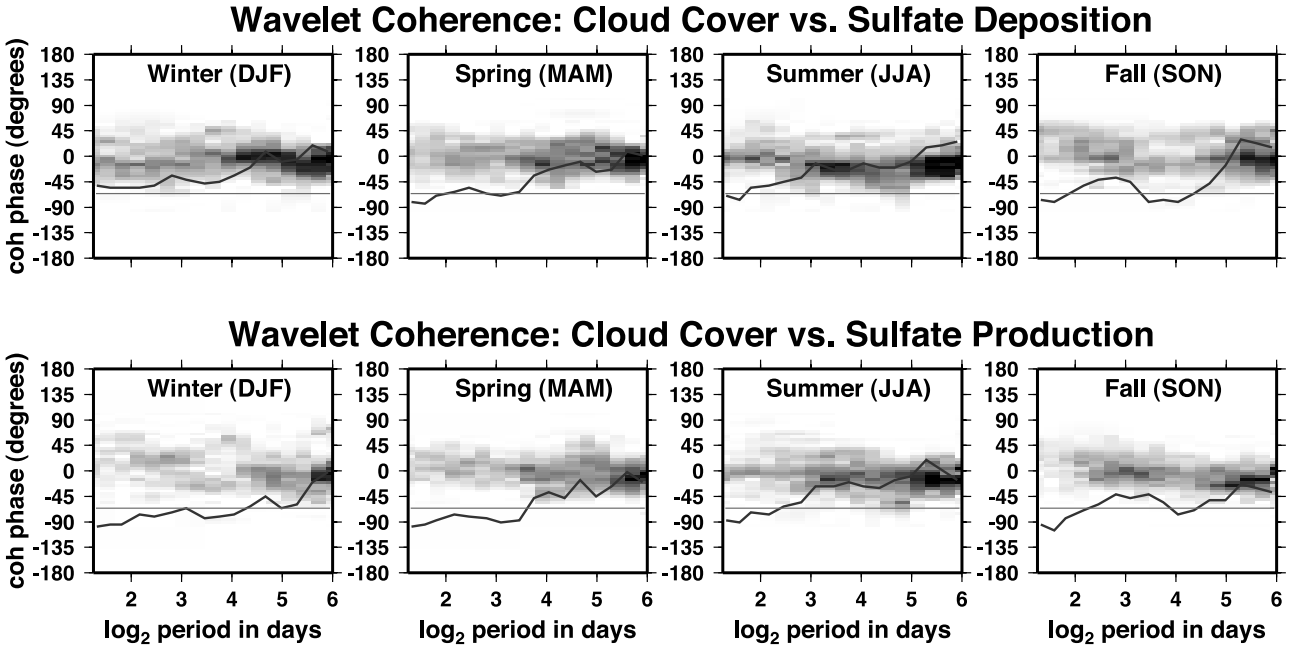

Figure 15. Coherence of model cloud cover with daily sulfate deposition (top) and with daily sulfate produced in-cloud (bottom). Results are from the European region.

observations. Furthermore, these models probably have excessive (APP) sulfate generation.

[47] Although the correction of our dissolved species scheme improved the coherence between clouds and sulfate, the resulting reduction in the sulfate burden creates a negative bias between the modeled and observed surface sulfate concentrations. Our standard model had very good agreement between model sulfate and observations at the surface [*Koch et al.*, 1999]. Now the model is low compared with observations, especially in Europe (where it was already too low). The average model bias (model-observations/observations, where the observations are from *Koch et al.* [1999]) decreases from ≈zero to about ≈−0.3 in source regions other than Europe; in Europe it decreases from −0.3 to −0.6. However, the model has excessive SO_2 at the surface, typically double the observations - more than enough to fix the sulfate bias. (Our standard model performance, with minimal sulfate bias but excessive SO_2, is typical of many global sulfur models; *Barrie et al.* [2001]). Therefore it appears that another mechanism for oxidizing SO_2 is required. Heterogeneous oxidation on aerosol particle surfaces, such as SO_2 oxidation by ozone on dust [e.g., *Usher et al.*, 2002] is a likely candidate: this would increase sulfate production, decrease $SO\{_2\}$, and since it would be most active in clear conditions it would enhance the negative sulfate-cloud correlations.

[48] Our study suggests that models ought to be producing more sulfate in clear conditions and less in cloudy conditions. This correction is likely to have implications for the indirect radiative forcing effect, since lower sulfate production near clouds should reduce the impact that sulfate can have on clouds. In order to test this, we repeated our standard and ''cloud budget'' simulations and included a simple parameterized relation between sulfate and cloud droplet number, similar to what was used by *Menon et al.* [2002] (but for sulfate only). The indirect (anthropogenic) radiative forcing decreased only slightly: it was -1.7 W m^{-2} for the standard case and -1.5 W m^{-2} for the simulation with the cloud budget. The impact on the direct anthropogenic radiative forcing is approximately proportional to the reduction in sulfate burden: the forcing decreases from -0.66 to -0.47 W m^{-2} for the standard and cloud-budget simulations, respectively. We note that including the (first) indirect effect in the simulations does not greatly affect the cloud-sulfate correlations. The second effect (where sulfate amount increases cloud lifetime) might, though it is likely to increase positive correlation rather than negative correlation.

[49] In addition to putting in a dissolved sulfate budget, we were also able to improve the cloud-sulfate anticorrelation by not allowing gas-phase sulfate production underneath clouds. Since our model imports its oxidants from another model, these off-line fields were affected by a different model's clouds. We tested the impact of this by setting the gas-phase production of sulfate equal to zero if a cloud was overhead. We found that this did strengthen the negative correlation between GPP sulfate and cloud cover. (However this improvement did not affect the correlation between clouds and total sulfate unless the dissolved budget decreased the aqueous-phase production relative to the gas-phase production.) Coupling the sulfate model to a full global chemistry model may further improve the anticorrelation. Since the aqueous-phase oxidant H_2O_2 is also affected by photochemistry (due to its photolysis, relation to OH, etc.), such coupling may impact the correlations for both phase-production pathways.

[50] In conclusion, we encourage the use of the observed anticorrelation between sulfate and clouds as a diagnostic test for global sulfate models. Furthermore, global aerosol and chemistry models need to verify that they are handling dissolution and evaporation correctly: that the dissolved species are only released from clouds as they evaporate. Fixing this in our model caused the ratio of the GPP sulfate burden to APP sulfate burden to increase from 1.3 to 2.

[51] **Acknowledgments.** This work was supported by the NASA Global Aerosol Climatology Program. J. Park was supported by NOAA grant Y770995. The EMEFS data utilized in this study were collected and prepared under the cosponsorship of the United States Environmental Protection Agency, the Atmospheric Environment Service, Canada, the Ontario Ministry of Environment, the Electric Power Research Institute, and the Florida Electric Power Coordinating Group.

References

Barrie, L. A., et al., A comparison of large-scale atmospheric sulfate aerosol models (COSAM): Overview and highlights, *Tellus, Ser. B*, *53*, 615–645, 2001.

Barth, M. C., P. J. Rasch, J. T. Kiehl, C. M. Benkovitz, and S. E. Schwartz, Sulfur chemistry in the National Center for Atmospheric Research Community Climate Model: Description, evaluation, features, and sensitivity to aqueous chemistry, *J. Geophys. Res.*, *105*, 1387–1415, 2000.

Bear, L. K., and G. L. Pavlis, Multi-channel estimation of time residuals from broadband seismic data using multi-wavelets, *Bull. Seismol. Soc. Am.*, *89*, 681–692, 1999.

Chin, M., R. B. Rood, S.-J. Lin, J.-F. Muller, and A. Thompson, Atmospheric sulfur cycle simulated in the global model GOCART: Model description and global properties, *J. Geophys. Res.*, *105*, 24,671–24,687, 2000.

Koch, D., D. Jacob, I. Tegen, D. Rind, and M. Chin, Tropospheric sulfur simulation and sulfate direct radiative forcing in the Goddard Institute for Space Studies general circulation model, *J. Geophys. Res.*, *104*, 23,799–23,822, 1999.

Lanzante, J., The leading modes of 10–30 day variability in the extratropics of the Northern Hemisphere during the cold season, *J. Atmos. Sci.*, *47*, 2115–2140, 1990.

Lilly, J., and J. Park, Multiwavelet spectral and polarization analysis of seismic records, *Geophys. J. Int.*, *122*, 1001–1021, 1995.

Lohmann, U., and G. Lesins, Stronger constraints on the anthropogenic indirect aerosol effect, *Science*, *298*, 1012–1015, 2002.

McNaughton, D. J., and R. J. Vet, Eulerian model evaluation field study (EMEFS): A summary of surface network measurments and data quality, *Atmos. Environ.*, *30*, 227–238, 1996.

Menon, S., A. D. Del Genio, D. Koch, and G. Tselioudis, GCM simulations of the aerosol indirect effect: Sensitivity to cloud parameterization and aerosol burden, *J. Atmos. Sci.*, *59*, 692–713, 2002.

Park, J., and M. E. Mann, Interannual temperature events and shifts in global temperature: A multiwavelet correlation approach, *Earth Interact.*, *4*, online paper 4-0001, 2000.

Park, J., F. L. Vernon III, and C. R. Lindberg, Frequency-dependent polarization analysis of high-frequency seismograms, *J. Geophys. Res.*, *92*, 12,664–12,674, 1987a.

Park, J., C. R. Lindberg, and F. L. Vernon III, Multitaper spectral analysis of high frequency seismograms, *J. Geophys. Res.*, *92*, 12,675–12,684, 1987b.

Penner, J. E., et al., Aerosols: Their direct and indirect effects, in *Climate Change 2001*: *The Scientific Basis*, edited by J. T. Houghton et al., pp. 289–348, Cambridge Univ. Press, New York, 2001.

Percival, D. B., and A. T. Walden, *Spectral Analysis for Physical Applications*, Cambridge Univ. Press, New York, 1993.

Rossow, W. B., and R. A. Schiffer, Advances in understanding clouds from ISCCP, *Bull. Am. Meteorol. Soc.*, *80*, 2261–2288, 1999.

Schaug, J., J. E. Hansen, K. Nodop, B. Ottar, and J. M. Pacyna, Summary report from the chemical co-ordinating center for the third phase of

EMEP, *EMEP/CC Rep. 3/87*, 160 pp., Norw. Inst. for Air Res., Lillestrom, 1987.

Schubert, S. D., A statistical-dynamical study of empirically determined modes of atmospheric variability, *J. Atmos. Sci.*, *42*, 3–17, 1985.

Schwartz, S. E., Harshvardhan, and C. M. Benkovitz, Influence of anthropogenic aerosol on cloud optical depth and albedo shown by satellite measurements and chemical transport modeling, *Proc. Nat. Acad. Sci.*, *99*, 1784–1789, 2002.

Stubenrauch, C. J., W. B. Rossow, F. Cheruy, A. Chdin, and N. A., Clouds as seen by satellite sounders (3I) and imagers (ISCCP). Part I. Evaluation of cloud parameters, *J. Clim.*, *12*, 2189–2213, 1999.

Thomson, D. J., Spectrum estimation and harmonic analysis, *IEEE Proc.*, *70*, 1055–1096, 1982.

Usher, C. R., H. Al-Hosney, S. Carlos-Cuellar, and V. H. Grassian, A laboratory study of the heterogeneous uptake and oxidation of sulfur dioxide on mineral dust particles, *J. Geophys. Res.*, *107*(D23), 4713, doi:10.1029/2002JD002051, 2002.

A. Del Genio and D. Koch, NASA Goddard Institute for Space Studies, Columbia University, 2880 Broadway, New York, NY 10025, USA. (dkoch@giss.nasa.gov)

J. Park, Department of Geology and Geophysics, Yale University, P.O. Box 208109 New Haven, CT 06520-8109, USA. (jeffrey.park@yale.edu)

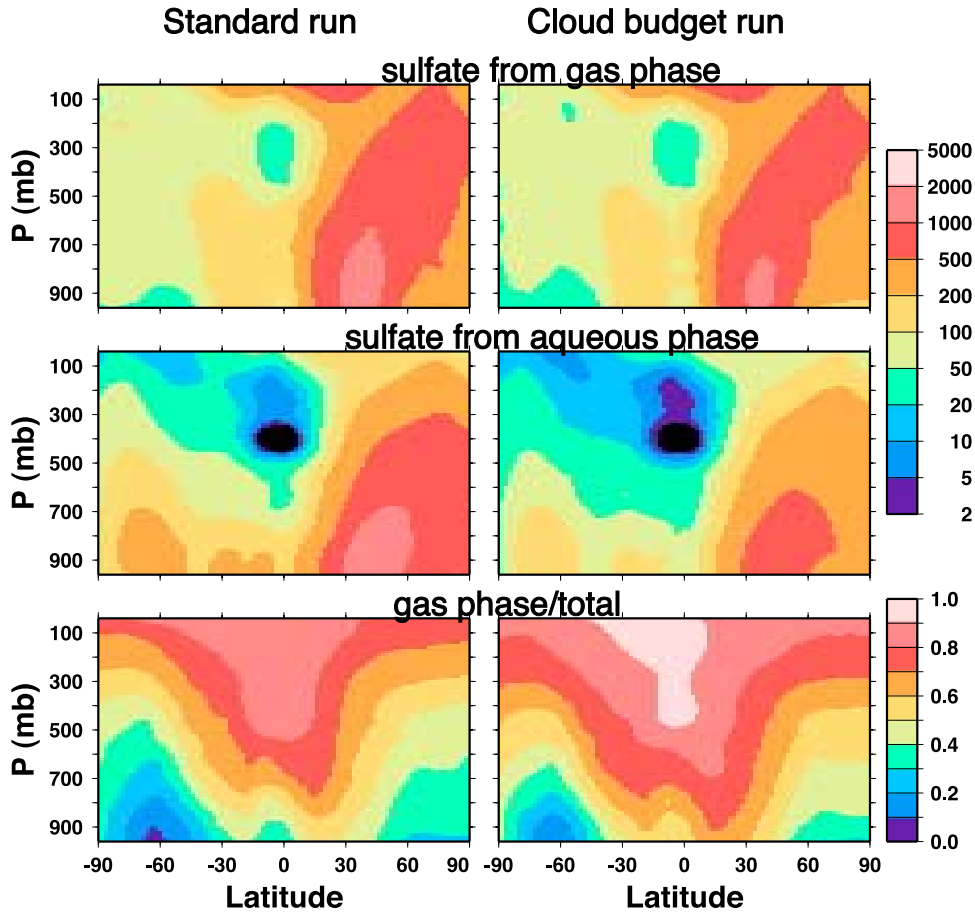

Figure 9. Zonal annual mean of the gas-phase produced sulfate, aqueous-produced sulfate, and gas-phase divided by the total sulfate for the standard run (1st column) and the cloud budget run (2nd column). The concentrations unit is ng m^{-3}.

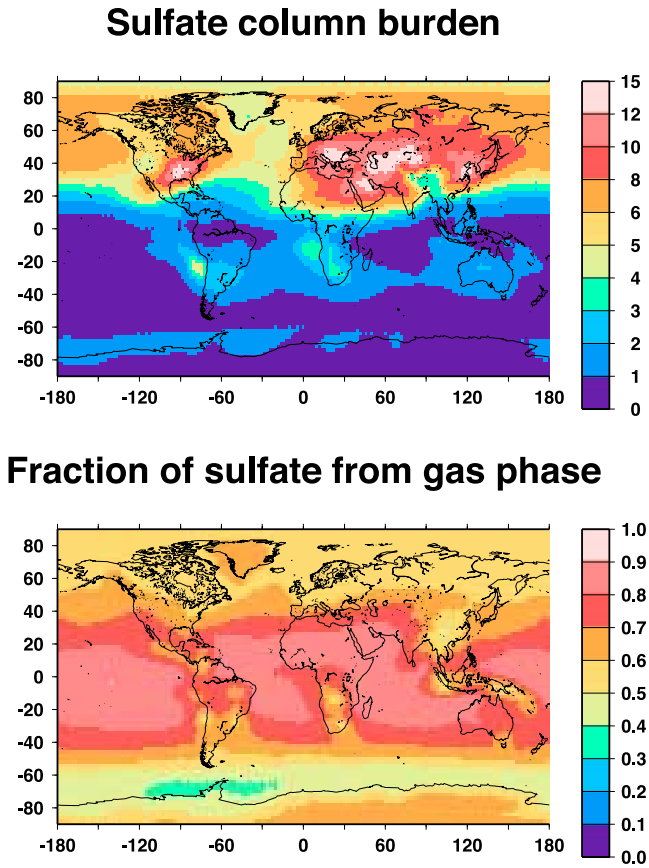

Figure 10. Annual average column burden of (total) sulfate (mg m^{-2}) at top. Below is the fraction derived from gas-phase production.